Hindawi Publishing Corporation
Journal of Nanomaterials
Volume 2016, Article ID 8032615, 10 pages
http://dx.doi.org/10.1155/2016/8032615

Research Article

Nanocomposites of Magnetite and Layered Double Hydroxide for Recyclable Chromate Removal

Gyeong-Hyeon Gwak,[1] Min-Kyu Kim,[1,2] and Jae-Min Oh[1]

[1]*Department of Chemistry and Medical Chemistry, College of Science and Technology, Yonsei University, Wonju, Gangwon-do 26493, Republic of Korea*
[2]*Future Industries Institute, Division of Information Technology, Engineering and Environment, University of South Australia, Mawson Lakes, SA 5095, Australia*

Correspondence should be addressed to Jae-Min Oh; jaemin.oh@yonsei.ac.kr

Received 7 April 2016; Revised 19 September 2016; Accepted 11 October 2016

Academic Editor: Yu-Lun Chueh

Copyright © 2016 Gyeong-Hyeon Gwak et al. This is an open access article distributed under the Creative Commons Attribution License, which permits unrestricted use, distribution, and reproduction in any medium, provided the original work is properly cited.

Nanocomposites containing magnetic iron oxide (magnetite) nanoparticles and layered double hydroxide (LDH) nanosheets were prepared by two different methods, exfoliation-reassembly and coprecipitation, for aqueous chromate adsorbent. According to X-ray diffraction, scanning electron microscopy, and atomic force microscopy, both nanocomposites were determined to develop different nanostructures; LDH nanosheets well covered magnetite nanoparticles with house-of-cards-like structure in exfoliation-reassembly method, while coprecipitation resulted in LDH particle formation along with magnetite nanoparticles. Zeta-potential measurement also revealed that the magnetite surface was effectively covered by LDH moiety in exfoliation-reassembly compared with coprecipitation. Time, pH, concentration dependent chromate adsorption tests, and magnetic separation experiments exhibited that both nanocomposites effectively adsorb and easily collect chromate. However, exfoliation-reassembly nanocomposite was determined to be slightly effective in chromate removal by ~10%. Chromate adsorbed nanocomposites could be regenerated by treating with bicarbonate and the regenerated nanocomposites preserved ~80% of chromate adsorption efficacy after three times of recycling.

1. Introduction

Fabrication of nanocomposites is a subject of great importance in developing functional nanomaterials such as catalysts [1], nanomedicines [2], electronic materials [3], and pollutant scavenger [4]. Various kinds of nanomaterial components, such as 0-dimensional particles [5], 1-dimensional tubes [6] or fibers [7], and 2-dimensional nanosheets [8], have been utilized to fabricate nanocomposites having various functionalities. Especially, 2-dimensional nanosheets have attracted interests to prepare nanocomposites for catalysts [9], electrodes [10], and energy storage [11], due to their high specific surface area, unusual physicochemical property resulting from anisotropic structure, and controllable compositions. Among the 2-dimensional nanosheets, layered double hydroxides, LDHs: $M(II)_{1-x}M(III)_x(OH)_2(A^{n-})_{x/n} \cdot mH_2O$, (M(II): divalent metal cation; M(III): trivalent metal cation; A^{n-}: anionic species with $n-$ charge, $0 < x < 1$; m: interlayer water quantity) have been widely studied in biomedical or environmental applications, as they have been reported to have biocompatibility [12], high anionic exchange capacity [13], tunable composition [14], and easy surface modification property [15]. As examples of LDH-based environmental remediation, nanoscale LDH reported by Goh et al. and hydrothermally prepared LDH reported by Wang et al. exhibited potential as chromate adsorbents with maximum efficacy of 33.8 and 12.15 mg Cr(VI)/g LDH, respectively [16, 17]. Yu et al. studied the removal of As(V) and Cr(VI) with MgAl-LDH whose three-dimensional hierarchical structure affected removal efficiency showing maximum ~150 mg Cr(VI)/g LDH and ~200 mg As(V)/g LDH [18].

Despite the high adsorption capacity of LDHs on pollutants, there still remain drawbacks for practical application: difficulties in collection after pollutant treatment and low

recyclability. Collection of adsorbents is a crucial factor in pollutant scavenger, especially for water treatment, in terms of preventing secondary pollution and recycling adsorbents. In this way, two strategies, introduction of magnetic properties to the LDHs [19–21] and fabrication of monoliths containing LDH moieties [22], have been suggested for easy collection. The first strategy, introduction of magnetic property to adsorbents, has been often reported due to effectiveness of magnetic separation. For this purpose, magnetic nanoparticles (Fe_3O_4) are generally utilized to fabricate nanocomposite with LDH. For instance, MgAl-LDH nanoparticles were *in situ* grown on magnetic $CoFe_2O_4$ nanoparticles through coprecipitation by Deng et al. [19]. The nanocomposite showed chromate removal efficacy of ~50 mg Cr(VI)/g adsorbent at 200 ppm chromate solution as well as preserved adsorption capacity up to 6 repeated adsorption tests. Similarly, ZnAl-LDH was introduced on magnetic Fe_3O_4 nanoparticles by coprecipitation [20], showing ~ 20 mg Cr(VI)/g adsorbent at 800 ppm chromate solution. Another literature reported MgAl-LDH/Fe_3O_4 nanocomposites prepared by coprecipitation, representing adsorption efficacy of ~60 mg dye (reactive red)/g adsorbent [21]. The other strategy of monolith fabrication has been scarcely reported. From our previous study, monolith-type nanocomposites having uniformly distributed MgAl-LDH nanoparticles in agarose scaffold have been developed for aqueous chromate removal, exhibiting ~100 mg Cr(VI)/g adsorbent [22].

In this study, we are going to prepare nanocomposites consisting of magnetic Fe_3O_4 nanoparticles and MgAl-LDH nanosheets for potential chromate removal in water treatment. For this purpose, we applied two different strategies in preparing nanocomposites: coprecipitation of MgAl-LDH on Fe_3O_4 nanoparticles as reported in other literatures [19–21] and exfoliation-reassembly of MgAl-LDH nanosheets on Fe_3O_4 nanoparticles. The former technique is widely studied in LDH-based adsorbent; on the other hand, there are a few literatures for the latter. In fact, exfoliation-reassembly is often utilized strategy in preparing nanoparticle-graphene composites for catalyst or energy storage materials [23, 24]. As LDH has 2-dimensional structure-like graphite, exfoliation-reassembly can be applied for nanocomposites of Fe_3O_4 nanoparticles and LDHs. Materials characterization such as crystal structure, particle morphology, and surface charge on two kinds of nanocomposites will be described. In order to examine chromate removal capability of both nanocomposites, contact time, pH, and concentration of chromate solutions were chosen as parameters. Furthermore, we collected nanocomposites by a magnet and repeated chromate adsorption test three times to evaluate recyclability of nanocomposites.

2. Materials and Methods

2.1. Materials. Magnesium nitrate hexahydrate ($Mg(NO_3)_2 \cdot 6H_2O$), aluminum nitrate nonahydrate ($Al(NO_3)_2 \cdot 9H_2O$), sodium bicarbonate ($NaHCO_3$), ferric chloride hexahydrate ($FeCl_3 \cdot 6H_2O$), ferrous chloride tetrahydrate ($FeCl_2 \cdot 4H_2O$), and potassium chromate (K_2CrO_4) were purchased from Sigma-Aldrich Co. LLC. (St. Louis, MO, USA). Sodium hydroxide (NaOH) and ammonia water (NH_4OH) were purchased from Duksan Pure Chemicals Company (Ansan, Korea). The deionized water (DI water) in all experiments was purified by Human Power II+ Water Purification System (Human Corporation, Seoul, Korea).

2.2. Preparation of Magnetite (Fe_3O_4) Nanoparticles. For the preparation of magnetite nanoparticles (Mag), mixed iron precursor (0.0263 mmol of $FeCl_3 \cdot 6H_2O$ and 0.0132 mmol of $FeCl_2 \cdot 4H_2O$) was dissolved in DI water (300 mL) with vigorous stirring at 50°C and then 32 mL of ammonia solution (6.64 M) was quickly added. After formation of black precipitates, the reactant was subjected to microwave treatment (2 minutes) for facilitated crystallization. Thus, obtained magnetite nanoparticles were centrifuged at 3500 rpm for 10 minutes, washed with DI water/acetone (1/1 v/v%) 3 times, and then dried in vacuo.

2.3. Preparation of Magnetite @ Layered Double Hydroxide (Mag@LDH) Nanocomposites with Two Different Methods ((1) Exfoliation-Reassembly (ER) and (2) Coprecipitation (CO)). First of all, magnetite powder (0.5 g) was dispersed in 10 mL DI water through ultrasonication for 20 minutes.

2.3.1. Mag@LDH Nanocomposites via Exfoliation-Reassembly Method (Mag@LDH-ER). MgAl-LDH precursor was synthesized by conventional coprecipitation. Briefly, mixed metal nitrate solution (0.063 mol of $Mg(NO_3)_2 \cdot 6H_2O$ and 0.0315 mol $Al(NO_3)_2 \cdot 9H_2O$) was titrated to pH of ~9.5 with alkaline solution (0.21 mol of NaOH) under vigorous stirring and N_2 purging. The white precipitates were aged for 24 hours and then washed 4 times utilizing centrifugation (10000 rpm, 10 minutes) and decarbonated water. Lyophilized MgAl-LDH powder (0.5 g) was dispersed in 500 mL formamide and stirred for 24 hours under N_2 purging in order to exfoliate LDH nanolayers as previously reported [25].

To introduce LDH nanosheets on magnetite, 10 mL of magnetite suspension (50 mg/mL) was put into 50 mL of $NaHCO_3$ solution (0.006 mol) and excess reactant was removed by centrifugation. Carbonate adsorbed magnetite suspension was then located in 50 mL of exfoliated LDH colloid (1 mg/mL) to introduce LDH nanosheets on carbonate adsorbed magnetite. The above two steps were repeated 10 times to increase LDH moiety on magnetite. The final product was washed thoroughly with DI water and lyophilized.

2.3.2. Mag@LDH Nanocomposites via Coprecipitation Method (Mag@LDH-CO). As-prepared magnetite suspension was sequentially treated with alkaline solution (0.0007 mol of $NaHCO_3$ and 0.0013 mol of NaOH in 15 mL) and mixed metal solution (0.0043 mol of $Mg(NO_3)_2 \cdot 6H_2O$ and 0.0022 mol $Al(NO_3)_3 \cdot 9H_2O$ in 20 mL) to promote coprecipitation of LDH on magnetite surface. At each step, centrifugation was utilized to separate solid part. The above steps were repeated 10 times to increase LDH moiety as in ER method. The obtained nanocomposite was collected by centrifugation and washed with DI water and lyophilized.

2.4. Characterization. The crystal structures of magnetite, MgAl-LDH, and two kinds of Mag@LDH nanocomposites were investigated with D2 phaser X-ray diffractometer (XRD) with Ni-filtered Cu-Kα radiation (λ = 1.5406 Å) manufactured by Bruker AXS (Billerica, MA, USA). To identify primary particle size and morphology, scanning electron microscopy (SEM; FEI Quanta 250 FEG, FEI Company, Hilsboro, OR, USA) measurement was carried out. Each sample was suspended in EtOH (0.01 wt/v%) and a drop of suspension was put on cleaned silicon wafer and dried in vacuum. Then, each sample was treated with Pt/Pd plasma for 1 minute and images were collected by 30 kV accelerated electron beam. For atomic force microscopy (AFM, NX10, Park Systems, Suwon, Korea), 0.00001 wt/v% of EtOH suspension was utilized and suspension was dropped on silicon wafer as described in SEM specimen preparation. Thickness and surface line profile of samples were obtained with in noncontact mode. Surface roughness (R_a) of each nanocomposite was calculated with Park system AFM XEI software. The zeta-potential values of pristine LDH and nanocomposites at pH 7 were investigated by ELSZ-1000 (Otsuka Electronics Co., LTD., Hirakata, Japan) with disposable cell at 25°C. Specific surface area was measured by N_2 adsorption-desorption isotherm with BELSORP-mini II (MicrotracBEL Corp., Osaka, Japan). Quantification of nanocomposite was carried out by inductively coupled plasma-optical emission spectrometer (ICP-OES; OPTIMA 7300 DV, Perkin Elmer, Waltham, MA, USA) after fully digesting sample with 10 M HCl solution.

2.5. Evaluation of Chromate Removal Efficacy on Mag@LDH Nanocomposites with Respect to Contact Time, pH, and Concentration of Chromate Solution. For the time-dependent chromate adsorption experiments, each nanocomposite (100 mg of Mag@LDH-ER or Mag@LDH-CO) was dispersed into 50 mL of chromate solution (50, 100, and 200 ppm of initial concentration) and then gently shaken by Orbital Shaker SH30 (FINEPCR, Gunpo, Korea) at 25°C. At the time points 0, 0.5, 1, 2, 3, 4, 6, 12, and 24 hours, nanocomposites were collected by magnetic separation and chromate concentration in supernatant was quantified with ultraviolet-visible spectrophotometer (UV-Vis; Shimadzu UV-1800, Shimadzu Corporation, Kyoto, Japan) at λ_{max} = 372 nm. In order to evaluate pH effect on chromate adsorption, initial pH of chromate solution (initial concentration of 50 ppm) was set to 2, 4, 5, 7, 9, and 11 utilizing 0.1 M HCl or 0.1 M NaOH solution, and then 100 mg of nanocomposites was dispersed into the solution. After 24 h, equilibrium pH and adsorbed amount of chromate was evaluated with pH meter and UV-Vis spectrophotometer, respectively.

2.6. Regeneration and Recyclability Test. To evaluate applicability of nanocomposites in practical water treatment, the regeneration and recyclability of nanocomposites in chromate removal were evaluated. In order to detach adsorbed chromate, chromate adsorbed nanocomposites were treated with $NaHCO_3$ solution (0.05 M, 50 mL) under stirring at room temperature for 6 hours. Thus, regenerated nanocomposites were collected by magnet and lyophilized. Then, the chromate adsorption experiment in Section 2.5 was repeated. Three cycles of adsorption test were carried out.

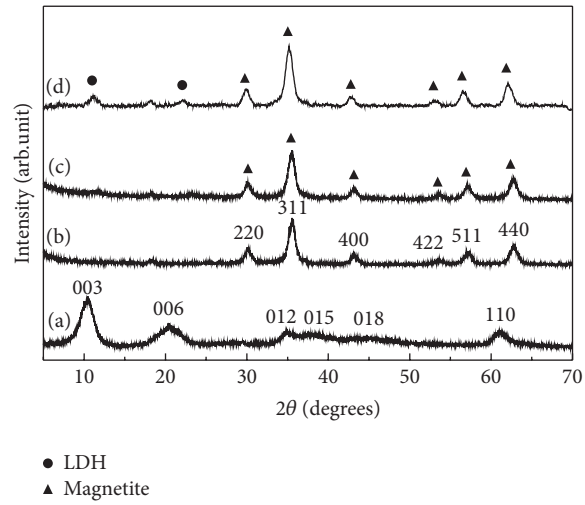

Figure 1: X-ray diffraction patterns of (a) MgAl-LDH, (b) magnetite, (c) Mag@LDH-ER, and (d) Mag@LDH-CO, respectively.

3. Result and Discussion

3.1. Characterization of Pristine LDH, Magnetite, and Two Nanocomposites, Mag@LDH-ER and Mag@LDH-CO. In order to identify the crystal structure of LDH, magnetite, and their nanocomposites, XRD patterns were obtained (Figure 1). In Figure 1(a), the pristine MgAl-LDH showed well-developed (*00l*) diffraction indicating stacking of 2-dimensional nanosheets. Along with (*00l*) peaks, lattice peaks such as (012), (015), (018), and (110) at 35.0, 38.1, 45.0, and 61.3° suggested successful development of hydrotalcite (JCPDS number 14-0191) phase as intended. The XRD pattern of Fe_3O_4 (Figure 1(b)) exhibited six characteristic peaks of inverse spinel structure of magnetite (JCPDS number 19-0629): (220), (311), (400), (422), (511), and (440) at 30.0, 35.1, 42.9, 54.0, 57.0, and 61.8°, respectively. The nanocomposite between magnetite and LDH through exfoliation-reassembly, Mag@LDH-ER, only exhibited peaks of magnetite without those of LDH (Figure 1(c)). Random stacking of delaminated LDH nanosheets on magnetite surface was thought to result in reduction of crystallinity. Similar phenomenon was reported elsewhere; exfoliation-reassembly of layered nanomaterials in the presence of nanoparticles forms house-of-cards structure resulting in the loss of layered XRD patterns [26, 27]. On the other hand, Mag@LDH-CO showed both X-ray diffraction patterns from LDH ((003) and (006): closed circles in Figure 1(d)) and magnetite ((220), (311), (400), (422), (511), and (440): closed triangles). It is expected that coprecipitation of LDH on magnetite resulted in ordered crystal growth rather than random stacking of nanosheets. XRD patterns containing both nanoparticle and LDH phase were reported in the synthesis of $CoFe_2O_4$@MgAl-LDH through coprecipitation [19].

According to SEM image (Figure 2), LDH and magnetite particles were determined to have irregular shape with

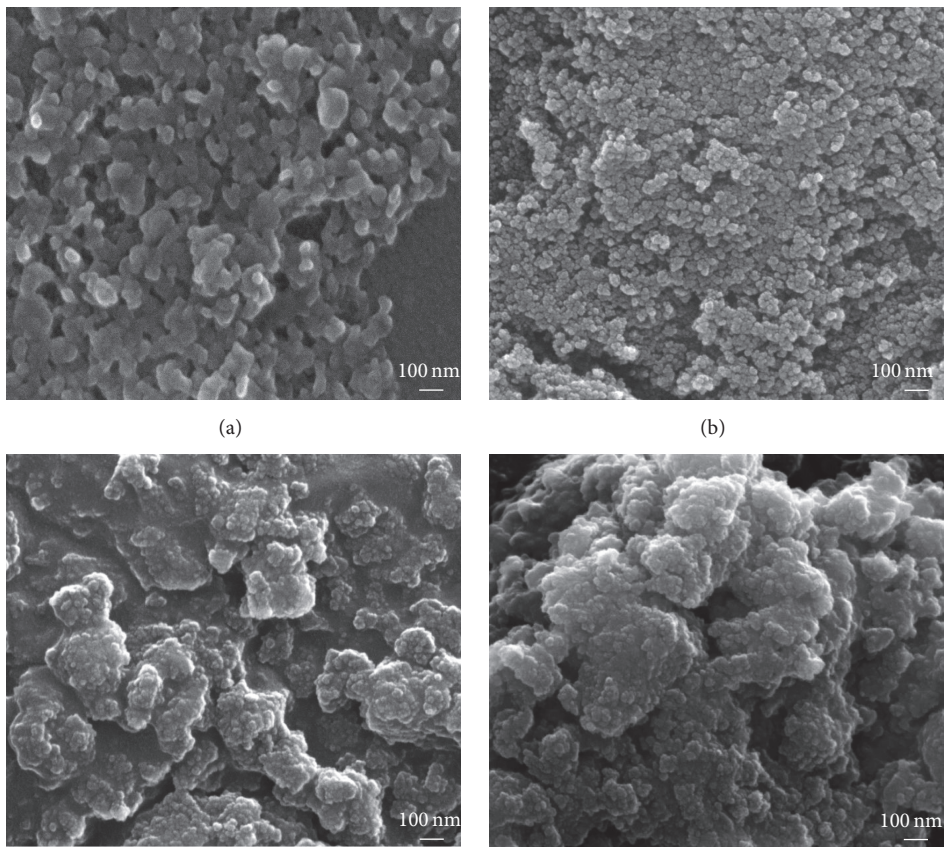

Figure 2: Scanning electron microscopic images of (a) MgAl-LDH, (b) magnetite, (c) Mag@LDH-ER, and (d) Mag@LDH-CO, respectively.

average diameters ~50 nm and ~30 nm, respectively. The surface morphology of Mag@LDH-ER was smooth compared with that of Mag@LDH-CO which showed agglomeration of small particles. Such smooth surface of nanoparticles has been reported in the nanocomposite between nanoparticles and nanosheets, suggesting house-of-card structure developed by reassembled nanosheets [26, 28].

In order to observe lateral size, thickness, and roughness of single particles, AFM images were obtained with diluted nanocomposites compared with SEM specimen (Figure 3). In Figures 3(a) and 3(b), Mag@LDH-ER had ~300 nm diameter and ~90 nm thickness, and Mag@LDH-CO had ~350 nm diameter and ~40 nm thickness. The surface of Mag@LDH-ER was determined to be less rough (R_a = 7.67 nm) than Mag@LDH-CO (R_a = 11.68 nm), which was corresponding to SEM observation. This result suggested that the LDH nanosheets covered magnetite nanoparticles in ER-nanocomposite, whereas both LDH and magnetite nanoparticles were homogeneously mixed in CO-nanocomposite.

3.2. Quantification and Physicochemical Property Evaluation on Nanocomposites. In order to determine chemical formulae of two nanocomposites, we quantified metal content through ICP-OES. As summarized in Table 1, the chemical formulae of Mag@LDH-ER and Mag@LDH-CO were $[Mg_{2.52}Al(OH)_{6.75}(CO_3)_{0.5}][Fe_3O_4]$ and $[Mg_{1.81}Al(OH)_{5.62}(CO_3)_{0.5}]_{0.82}[Fe_3O_4]$, respectively, suggesting that slightly more LDH moiety was introduced by ER method. However, active adsorption site (Al^{3+}) per g nanocomposite was fairly similar for Mag@LDH-ER and Mag@LDH-CO. Specific surface area values were determined: 97.4 and 122.4 m^2/g for Mag@LDH-ER and Mag@LDH-CO, respectively.

The average zeta-potential values were +20.78 and +9.52 mV for Mag@LDH-ER and Mag@LDH-CO, showing more positive surface charge on ER-nanocomposite. As shown in Figure 4, pristine LDH had highly positive charge (+42.21 mV), while magnetite had negative charge (−34.33 mV). Supposing that the LDHs sufficiently cover magnetite surface, the negative surface charge of magnetite would be camouflaged. The zeta-potential graph of Mag@LDH-CO lay from −50 to +50 mV, clearly showing negatively charged region. In ER method, LDH nanosheets covered magnetite surface effectively to form particle-plate nanocomposite, as the nanosheets had larger lateral dimension (~50 nm) than magnetite's diameter (~30 nm). On the other hand, LDH nanoparticles formed in CO method were thought to be more particle-like rather than plate, which

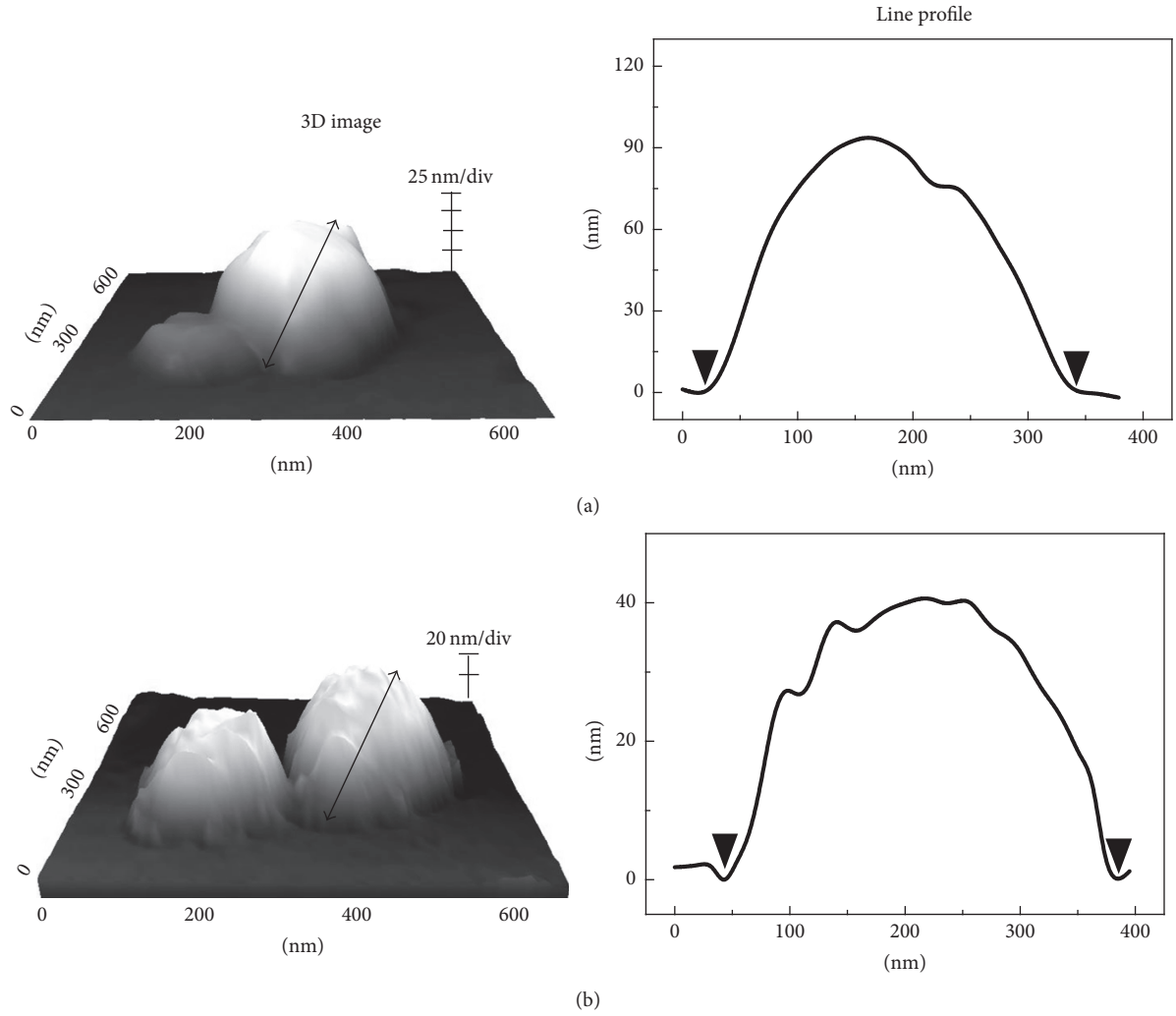

Figure 3: Atomic force microscopic 3D images and corresponding line profiles of (a) Mag@LDH-ER and (b) Mag@LDH-CO, respectively.

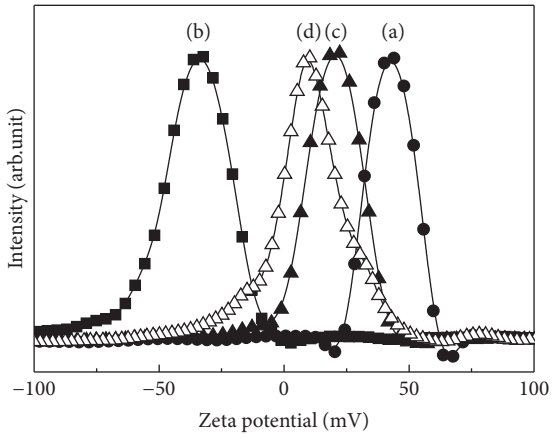

Figure 4: Zeta-potential distribution patterns for (a) MgAl-LDH, (b) magnetite, (c) Mag@LDH-ER, and (d) Mag@LDH-CO.

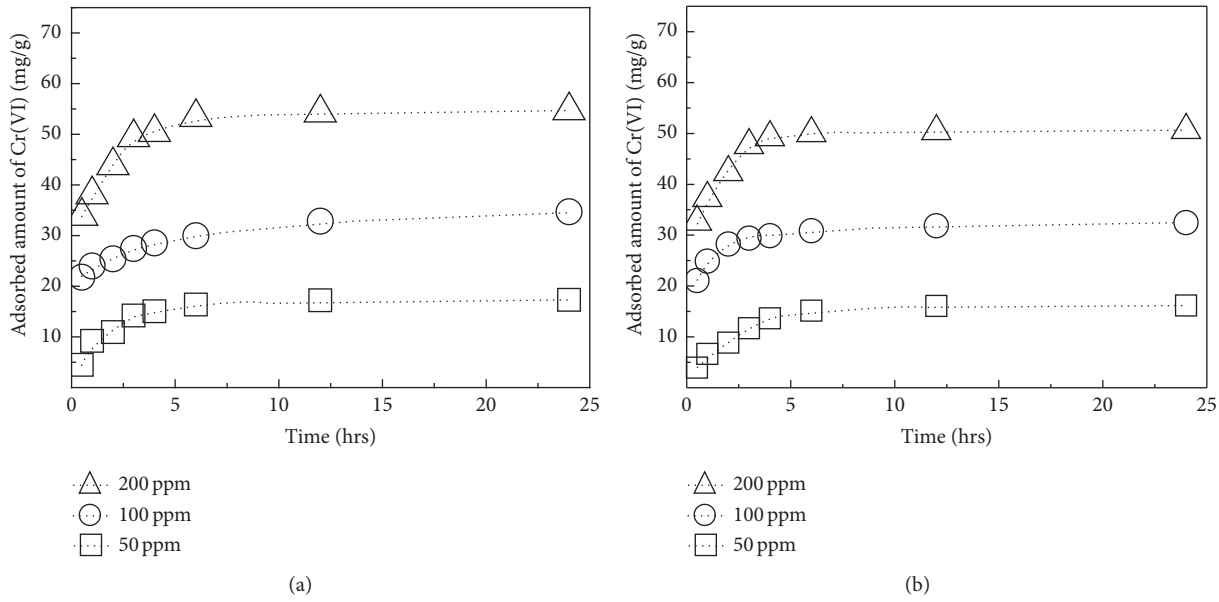

Figure 5: Time-dependent chromate adsorption amount (mg chromate/g nanocomposite) at different initial chromate concentrations for (a) Mag@LDH-ER and (b) Mag@LDH-CO. The experiments were carried out at pH ~ 7.

Table 1: Quantification results and physicochemical properties of (a) Mag@LDH-ER and (b) Mag@LDH-CO.

Sample	Chemical formulae	Al^{3+}/nanocomposite (mol/g)	Specific surface area (m^2/g)	Zeta potential (mV)
(a)	$[Mg_{2.52}Al(OH)_{6.75}(CO_3)_{0.5}][Fe_3O_4]$	0.0022	97.4	+20.78
(b)	$[Mg_{1.81}Al(OH)_{5.62}(CO_3)_{0.5}][Fe_3O_4]_{1.22}$	0.0021	122.4	+9.52

resulted in particle-particle nanocomposite between LDH and magnetite. The evolution of LDH phases in XRD (Figure 1), rough surface (Figures 2 and 3), and larger specific surface area of Mag@LDH-CO also corresponded to this hypothesis.

3.3. Evaluation of Chromate Removal Efficacy of Nanocomposites (Mag@LDH-ER and Mag@LDH-CO). Time-dependent chromate removal test at different initial chromate concentrations (50, 100, and 200 ppm) was carried out for both nanocomposites and the results were displayed in Figure 5. The amount of adsorbed chromate increased according to the initial concentration of chromate. Saturated chromate removal efficacy of Mag@LDH-ER at equilibrium time (~24 hours) was 17.30, 34.71, and 54.68 mg Cr(VI)/g nanocomposite at 50, 100, and 200 ppm of chromate solution, respectively. The removal efficacy of Mag@LDH-CO at 24 h was determined to 16.07, 31.83, and 50.65 mg Cr(VI)/g nanocomposite at 50, 100, and 200 ppm of chromate, respectively. These results showed that the chromate removal efficacies of current nanocomposites were comparable or higher than previous reports as we described in Introduction [16, 17]. Furthermore, considering that the current nanocomposites have less than 50 wt% of LDH content, the chromate removal ability of LDH moiety in the nanocomposites is thought fairly high.

Although the time and concentration dependent chromate removal of two nanocomposites seemed similar, Mag@LDH-ER had approximately 10% larger chromate adsorption ability than Mag@LDH-CO (Table 2). It should be noted that, in the adsorption of LDH, both positive charge sites (Al^{3+}) and specific surface area values affected adsorption ability. From Table 1, we could calculate that Mag@LDH-CO had 5% less positive sites but 25% larger surface area per gram than Mag@LDH-ER. Thus, the higher adsorption was expected with Mag@LDH-CO, which was not the case in our study. This discrepancy could be explained by the different nanostructure and surface charge of two nanocomposites. Mag@LDH-ER, in which LDH well covered magnetite nanoparticles to have more positive surface charge, facilitated chromate approach to the nanocomposites compared to Mag@LDH-CO, resulting in better chromate adsorption.

To analyze the adsorption rate in the overall adsorption process of chromate onto nanocomposites, the experiment data was fitted using pseudo-first-order (1) and pseudo-second-order kinetic (2) [29] models, with the respective kinetics equations defined as follows:

$$\log\left(Q_e - Q_t\right) = \log Q_e - \frac{k_1}{2.303}t, \tag{1}$$

$$\frac{t}{Q_t} = \frac{1}{k_2 Q_e^2} + \frac{1}{Q_e}t. \tag{2}$$

(Q_e (mg/g) and Q_t (mg/g) are the amounts of chromate adsorbed at equilibrium time at any instant of time, t, resp.,

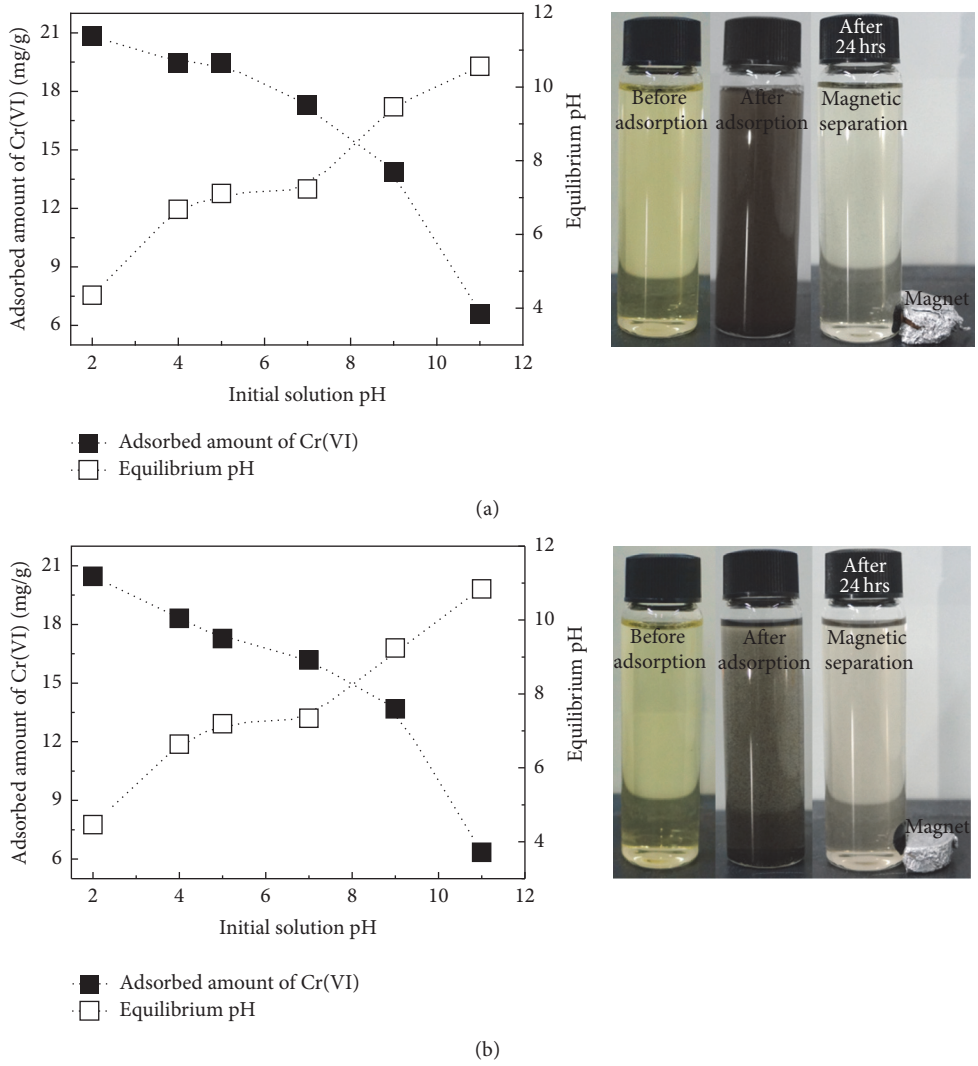

Figure 6: Effect of initial solution pH on Cr(VI) adsorption and equilibrium pH for (a) Mag@LDH-ER and (b) Mag@LDH-CO. The experiments were carried out at initial chromate concentration of 50 ppm. The photographs in the right side represent adsorption and separation of each nanocomposite at pH ~ 7.

and k_1 (min^{-1}) and k_2 ($g(mg^{-1}\ min^{-1})$) are the rate constant of pseudo-first-order and pseudo-second-order kinetic model, resp.) The kinetic constants, k_1 and k_2, were determined from the slope of the linear plot of $\log(Q_e - Q_t)$ versus t and t/Q_t versus t, respectively. As represented in Table 2, the correlation coefficient (R^2) obtained from the pseudo-second-order kinetic model ($R^2 \geq 0.99$) was higher than that obtained from the pseudo-first-order model (R^2 was in the range of 0.91–0.98), suggesting that the adsorption of chromate onto adsorbents followed pseudo-second-order kinetic. According to literatures [29], the rate determining step of LDH is chemical adsorption through sharing or exchange of electrons between the adsorbents and chromate rather than physical adsorption. k_2 values were similar for both nanocomposites, suggesting that the adsorption of both nanocomposites were mediated by LDH-based chromate adsorption. However, the overall adsorption amount was thought to be dependent on zeta-potential value of nanocomposite, showing better adsorption on Mag@LDH-ER. According to time-dependent chromate adsorption study, we verified that the adsorption reached equilibrium after 24 hours.

Solution pH plays an important role in chromate adsorption owing to its effect not only on the degree of chromate speciation [30] but also on surface charge of the adsorbents. Figure 6 showed the results of chromate adsorption by nanocomposites with the initial solution pH ranging from ~2 to ~11 at initial solution concentration of 50 ppm. Equilibrium pH was fairly similar to initial pH above pH 7 and lower than initial value below pH 7. The pH raising at acidic condition was attributed to the basic property of LDH moiety. The amount of chromate removal was highly dependent on pH showing gradual decrease from 20.83 (pH ~ 2) to 6.57 mg/g (pH ~ 11) for Mag@LDH-ER and 20.45 (pH ~ 2) to 6.34 mg/g (pH ~ 11) for Mag@LDH-CO. Chromate can have various speciation like H_2CrO_4, $HCrO_4^-$, CrO_4^{2-}, and $Cr_2O_7^{2-}$; at low pH, $HCrO_4^-$ and $Cr_2O_7^{2-}$ are prevalent, while CrO_4^{2-} becomes

Table 2: Adsorption parameters and kinetic fitting results for (a) Mag@LDH-ER and (b) Mag@LDH-CO.

Sample	Initial concentration (ppm)	Adsorbed amount (mg Cr(VI)/g nanocomposite)	Pseudo-first-order		Pseudo-second-order	
	C_0	Q_e	k_1	R^2	k_2	R^2
(a)	50	17.30	0.003	0.96	0.052	0.99
	100	34.71	0.001	0.98	0.030	0.99
	200	54.68	0.002	0.93	0.018	0.99
(b)	50	16.07	0.003	0.96	0.053	0.99
	100	31.83	0.002	0.96	0.031	0.99
	200	50.65	0.003	0.91	0.019	0.99

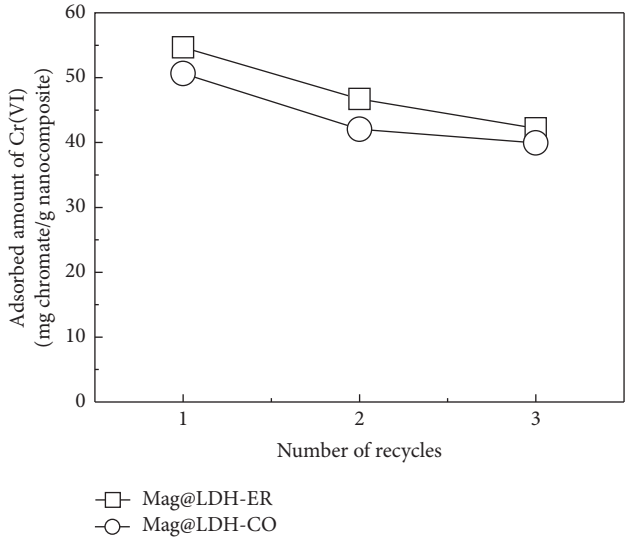

Figure 7: Adsorbed amount of chromate on Mag@LDH-ER and Mag@LDH-CO at each recycling step. The experiments were carried out at initial chromate concentration of 200 ppm, pH ~ 7.

majority above pH 7 [30]. According to the isoelectric point ~9 of LDH [31], the anionic adsorption ability of LDH could be significantly affected by the pH condition. At low pH, less negative chromate species like $HCrO_4^-$ exists, but highly positive surface charge of LDH can result in facilitated adsorption. The pH dependent property of chromate and LDH resulted in efficient chromate removal at low pH region. From the photographs in Figure 6, it was clearly observed that the adsorbent was quickly separated from the aqueous solution by an external magnet after adsorption process. Compared to previous reports [19, 20], these results showed that prepared nanocomposites can be considered to use as a good chromate removal materials with maintaining their magnetic property.

In order to utilize prepared nanocomposites into actual application, chromate adsorption test was repeated three times. For recycling nanocomposites, chromate was desorbed from the nanocomposites by treating in $NaHCO_3$ solution (0.05 M, 50 mL) under stirring at room temperature for 6 hours. From Figure 7, it was found that the adsorbed amount of chromate on nanocomposite remained high (~80%) even in the third-regeneration cycle, although the adsorbed amount was slightly higher in Mag@LDH-ER at every recycling stage. This result suggested that the nanocomposites have the potential use as recyclable chromate scavenger in water treatment.

4. Conclusion

Nanocomposites consisting of magnetite nanoparticles and LDH nanosheets were prepared via two different methodologies. One is reassembly of exfoliated LDH nanosheets on magnetite nanoparticles (ER), and the other is generation of LDH on magnetite nanoparticles (CO), termed as Mag@LDH-ER and Mag@LDH-CO, respectively. According to XRD, SEM, AFM, and zeta-potential measurement, it was identified that LDH nanosheets covered surface of magnetite effectively in Mag@LDH-ER nanocomposite. On the other hand, LDH nanoparticles formed in CO method coexist with magnetite to make larger lumps than pristine particles. For evaluation of chromate removal efficacy, contact time, pH, and concentration of chromate solutions were set as adsorption parameters. Mag@LDH-ER and Mag@LDH-CO showed maximum adsorption amount of 54.68 and 50.65 mg Cr(VI)/g nanocomposite after 24 hours, suggesting slightly enhanced adsorption efficacy of ER-nanocomposite. Both nanocomposites showed similar pH dependent chromate adsorption behavior, decreasing adsorption upon increasing pH. Kinetic and pH dependent studies revealed that LDH was the major adsorption sites for chromate in the nanocomposites. Easy collection and regeneration of both Mag@LDH nanocomposites were shown and adsorption capability was preserved ~80% during three times of recycling. In conclusion, we could suggest that magnetite@LDH nanocomposites prepared by either coprecipitation or exfoliation-reassembly can be applied to the environmental remediating scavenger with recyclability.

Competing Interests

The authors declare that they have no competing interests.

Authors' Contributions

Gyeong-Hyeon Gwak and Min-Kyu Kim contributed equally to this work.

Acknowledgments

This work was supported by a grant from Postharvest Research Project (PJ01050201) of Rural Development Administration (RDA), Nuclear R&D Program (2015M2B2A4031430), and International Research & Development Program (NRF-2014K1A3A1A21001297) through National Research Foundation of Korea (NRF) funded by the Ministry of Science, ICT and Future Planning.

References

[1] M. Shokouhimehr, Y. Piao, J. Kim, Y. Jang, and T. Hyeon, "A magnetically recyclable nanocomposite catalyst for olefin epoxidation," *Angewandte Chemie*, vol. 119, no. 37, pp. 7169–7173, 2007.

[2] O. V. Salata, "Applications of nanoparticles in biology and medicine," *Journal of Nanobiotechnology*, vol. 2, no. 1, article 3, 2004.

[3] F. Croce, G. B. Appetecchi, L. Persi, and B. Scrosati, "Nanocomposite polymer electrolytes for lithium batteries," *Nature*, vol. 394, no. 6692, pp. 456–458, 1998.

[4] H. Zhao and K. L. Nagy, "Dodecyl sulfate-hydrotalcite nanocomposites for trapping chlorinated organic pollutants in water," *Journal of Colloid and Interface Science*, vol. 274, no. 2, pp. 613–624, 2004.

[5] Y. Zheng, Y. Zheng, and R. Ning, "Effects of nanoparticles SiO_2 on the performance of nanocomposites," *Materials Letters*, vol. 57, no. 19, pp. 2940–2944, 2003.

[6] M. Moniruzzaman and K. I. Winey, "Polymer nanocomposites containing carbon nanotubes," *Macromolecules*, vol. 39, no. 16, pp. 5194–5205, 2006.

[7] J. A. Prince, G. Singh, D. Rana, T. Matsuura, V. Anbharasi, and T. S. Shanmugasundaram, "Preparation and characterization of highly hydrophobic poly(vinylidene fluoride)—clay nanocomposite nanofiber membranes (PVDF-clay NNMs) for desalination using direct contact membrane distillation," *Journal of Membrane Science*, vol. 397, pp. 80–86, 2012.

[8] L. M. Veca, M. J. Meziani, W. Wang et al., "Carbon nanosheets for polymeric nanocomposites with high thermal conductivity," *Advanced Materials*, vol. 21, no. 20, pp. 2088–2092, 2009.

[9] S. I. Shin, A. Go, I. Y. Kim, J. M. Lee, Y. Lee, and S.-J. Hwang, "A beneficial role of exfoliated layered metal oxide nanosheets in optimizing the electrocatalytic activity and pore structure of Pt-reduced graphene oxide nanocomposites," *Energy and Environmental Science*, vol. 6, no. 2, pp. 608–617, 2013.

[10] J. M. Lee, I. Y. Kim, S. Y. Han, T. W. Kim, and S.-J. Hwang, "Graphene nanosheets as a platform for the 2D ordering of metal oxide nanoparticles: mesoporous 2D aggregate of anatase TiO_2 nanoparticles with improved electrode performance," *Chemistry-A European Journal*, vol. 18, no. 43, pp. 13800–13809, 2012.

[11] S.-M. Paek, E. Yoo, and I. Honma, "Enhanced cyclic performance and lithium storage capacity of SnO_2/graphene nanoporous electrodes with three-dimensionally delaminated flexible structure," *Nano Letters*, vol. 9, no. 1, pp. 72–75, 2009.

[12] J.-H. Choy, S.-J. Choi, J.-M. Oh, and T. Park, "Clay minerals and layered double hydroxides for novel biological applications," *Applied Clay Science*, vol. 36, no. 1–3, pp. 122–132, 2007.

[13] J.-H. Choy, "Intercalative route to heterostructured nanohybrid," *Journal of Physics and Chemistry of Solids*, vol. 65, no. 2-3, pp. 373–383, 2004.

[14] H. Yang, C. Liu, D. Yang, H. Zhang, and Z. Xi, "Comparative study of cytotoxicity, oxidative stress and genotoxicity induced by four typical nanomaterials: the role of particle size, shape and composition," *Journal of Applied Toxicology*, vol. 29, no. 1, pp. 69–78, 2009.

[15] J.-M. Oh, S.-J. Choi, G.-E. Lee, S.-H. Han, and J.-H. Choy, "Inorganic drug-delivery nanovehicle conjugated with cancer-cell-specific ligand," *Advanced Functional Materials*, vol. 19, no. 10, pp. 1617–1624, 2009.

[16] K.-H. Goh, T.-T. Lim, and Z. Dong, "Application of layered double hydroxides for removal of oxyanions: a review," *Water Research*, vol. 42, no. 6-7, pp. 1343–1368, 2008.

[17] W. Wang, J. Zhou, G. Achari, J. Yu, and W. Cai, "Cr(VI) removal from aqueous solutions by hydrothermal synthetic layered double hydroxides: adsorption performance, coexisting anions and regeneration studies," *Colloids and Surfaces A: Physicochemical and Engineering Aspects*, vol. 457, no. 1, pp. 33–40, 2014.

[18] X.-Y. Yu, T. Luo, Y. Jia et al., "Three-dimensional hierarchical flower-like Mg–Al-layered double hydroxides: highly efficient adsorbents for As(V) and Cr(VI) removal," *Nanoscale*, vol. 4, no. 11, pp. 3466–3474, 2012.

[19] L. Deng, Z. Shi, and X. Peng, "Adsorption of Cr(vi) onto a magnetic $CoFe_2O_4$/MgAl-LDH composite and mechanism study," *RSC Advances*, vol. 5, no. 61, pp. 49791–49801, 2015.

[20] L.-G. Yan, K. Yang, R.-R. Shan, H.-Q. Yu, and B. Du, "Calcined ZnAl- and Fe_3O_4/ZnAl-layered double hydroxides for efficient removal of Cr(VI) from aqueous solution," *RSC Advances*, vol. 5, no. 117, pp. 96495–96503, 2015.

[21] R.-R. Shan, L.-G. Yan, K. Yang et al., "Magnetic Fe_3O_4/MgAl-LDH composite for effective removal of three red dyes from aqueous solution," *Chemical Engineering Journal*, vol. 252, pp. 38–46, 2014.

[22] G.-H. Gwak, M.-K. Kim, and J.-M. Oh, "Composites of quasi-colloidal layered double hydroxide nanoparticles and agarose hydrogels for chromate removal," *Nanomaterials*, vol. 6, no. 2, article 25, 2016.

[23] S. J. R. Prabakar, Y.-H. Hwang, E.-G. Bae et al., "SnO_2/Graphene Composites with self-assembled alternating oxide and amine layers for high li-storage and excellent stability," *Advanced Materials*, vol. 25, no. 24, pp. 3307–3312, 2013.

[24] S.-M. Paek, J.-U. Jang, S.-J. Hwang, and J.-H. Choy, "Exfoliation–restacking route to Au nanoparticle-clay nanohybrids," *Journal of Physics and Chemistry of Solids*, vol. 67, no. 5-6, pp. 1020–1023, 2006.

[25] F. Leroux, M. Adachi-Pagano, M. Intissar, S. Chauvière, C. Forano, and J.-P. Besse, "Delamination and restacking of layered doublehydroxides," *Journal of Materials Chemistry*, vol. 11, no. 1, pp. 105–112, 2001.

[26] X.-L. Wu, L. Wang, C.-L. Chen, A.-W. Xu, and X.-K. Wang, "Water-dispersible magnetite-graphene-LDH composites for efficient arsenate removal," *Journal of Materials Chemistry*, vol. 21, no. 43, pp. 17353–17359, 2011.

[27] J. M. Lee, J. L. Gunjakar, Y. Ham, I. Y. Kim, K. Domen, and S.-J. Hwang, "A linker-mediated self-assembly method to couple isocharged nanostructures: layered double hydroxide–CdS nanohybrids with high activity for visible-light-induced H_2 generation," *Chemistry—A European Journal*, vol. 20, no. 51, pp. 17004–17010, 2014.

[28] H. Li, L. Deng, G. Zhu, L. Kang, and Z.-H. Liu, "Fabrication and capacitance of Ni^{2+}-Fe^{3+} LDHs/MnO_2 layered nanocomposite

via an exfoliation/reassembling process," *Materials Science and Engineering B: Solid-State Materials for Advanced Technology*, vol. 177, no. 1, pp. 8–13, 2012.

[29] W. Rudzinski and W. Plazinski, "Kinetics of solute adsorption at solid/solution interfaces: a theoretical development of the empirical pseudo-first and pseudo-second order kinetic rate equations, based on applying the statistical rate theory of interfacial transport," *Journal of Physical Chemistry B*, vol. 110, no. 33, pp. 16514–16525, 2006.

[30] I. García-Sosa and M. Olguín, "Comparison between the Cr (VI) adsorption by hydrotalcite and hydrotalcite-gibbsite compounds," *Separation Science and Technology*, vol. 50, no. 17, pp. 2631–2638, 2015.

[31] Y. Zhang and J. R. G. Evans, "Alignment of layered double hydroxide platelets," *Colloids and Surfaces A: Physicochemical and Engineering Aspects*, vol. 408, pp. 71–78, 2012.


Journal of
Nanotechnology

International Journal of
Corrosion

International Journal of
Polymer Science

Smart Materials
Research

Journal of
Composites

BioMed
Research International
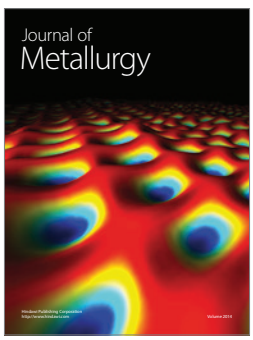
Journal of
Metallurgy

Journal of
Materials

Hindawi
Submit your manuscripts at
http://www.hindawi.com
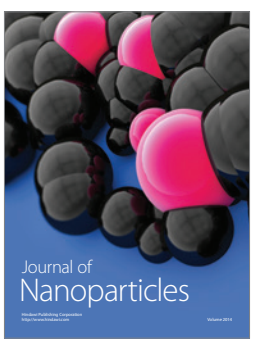
Journal of
Nanoparticles
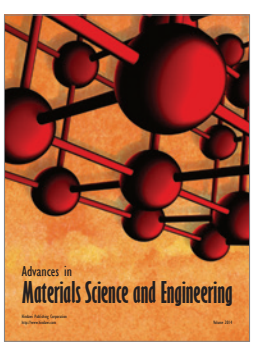
Advances in
Materials Science and Engineering
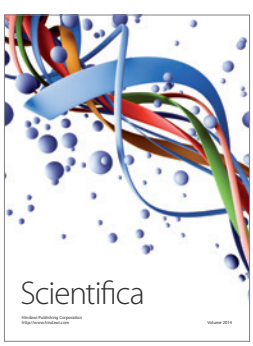
Scientifica
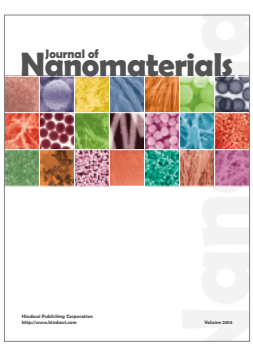
Journal of
Nanomaterials

The Scientific
World Journal

International Journal of
Biomaterials
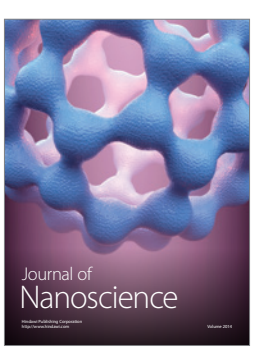
Journal of
Nanoscience

Journal of
Coatings
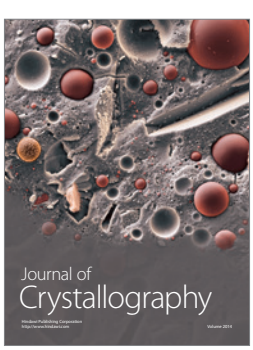
Journal of
Crystallography

Journal of
Ceramics
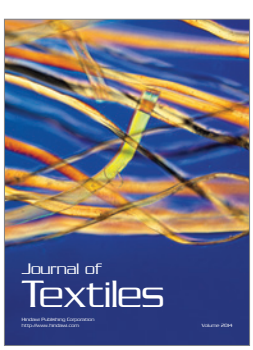
Journal of
Textiles